Available online at www.sciencedirect.com
SCIENCE DIRECT®
Biochemical and Biophysical Research Communications 323 (2004) 185–191
BBRC
www.elsevier.com/locate/ybbrc

Structural evidence for guanidine–protein side chain interactions: crystal structure of CutA from *Pyrococcus horikoshii* in 3 M guanidine hydrochloride☆,☆☆

Yoshikazu Tanaka[a], Kouhei Tsumoto[a,*], Mitsuo Umetsu[a], Takeshi Nakanishi[a], Yoshiaki Yasutake[b], Naoki Sakai[b], Min Yao[b], Isao Tanaka[b], Tsutomu Arakawa[c,*], Izumi Kumagai[a]

[a] *Department of Biomolecular Engineering, Graduate School of Engineering, Tohoku University, Aobayama 07, Aoba-ku, Sendai 980-8579, Japan*
[b] *Division of Biological Sciences, Graduate School of Science, Hokkaido University, Sapporo 060-0810, Japan*
[c] *Alliance Protein Laboratories, Thousand Oaks, CA 91360, USA*

Received 22 May 2004

Abstract

This study was carried out to investigate the structural perturbation of the protein's local structure by the denaturants under non-denaturing conditions. Crystal structure of CutA from an archaeon *Pyrococcus horikosii* (*Pho*CutA), a heavy-metal binding protein, was determined at 1.6-Å resolution in the presence of 3 M guanidine HCl (GdnHCl). Native *Pho*CutA has a large number of short intramolecular hydrogen bonds and salt bridges on the protein surface, of which greater than 90% of hydrogen bonds and all salt bridges were retained in 3 M GdnHCl. Hydrogen bonds that disappeared in the GdnHCl crystal structure were mainly located on the protein surface, especially around the structurally perturbed loop, suggesting interactions between peptide groups and GdnHCl. Only a few $GdnH^+$ ions were observed in the crystal structure, although none at the surface, of the protein. Two $GdnH^+$ ions were observed in the center of the trimeric structure, replacing water molecules, and were hydrogen bonded with Asp84 and Asp86 of each chain. The exterior loop from Tyr39 to Lys44, including Trp40–Trp41, was perturbed structurally. Decreases in temperature factors were observed in β strand 5 and the N terminus of helix 3. These results suggest the specific bindings of $GdnH^+$ with some acidic residues and the non-specific bindings around Trp residues and peptide groups on the protein surface and that binding of GdnHCl to the native protein is limited, resulting in local structural perturbation.

Keywords: Guanidine; Interaction; Denaturant; Crystal structure; Structural perturbation; Archaeon

Protein structure is now known as an ensemble of many fluctuating micro-states. Increased temperature or chemical denaturant can alter this ensemble even before the co-operative unfolding. Chemical denaturation by guanidine HCl (GdnHCl) or urea is widely used as a method for studying the folding and stability of

☆ *Abbreviations:* GdnHCl, guanidine hydrochloride; SDS, sodium dodecyl sulfate; PAGE, polyacrylamide gel electrophoresis; *Pho*CutA, *Pyrococcus horikoshii* CutA; CD, circular dichroism.

☆☆ This work was supported in part by a grant from the National Project on Protein Structural and Functional Analyses from the Ministry of Education, Culture, Sports, Science and Technology of Japan. It was also partially supported by a Grant-in-Aid for the COE project, Giant Molecules and Complex Systems, 2002, from the Ministry of Education, Culture, Sports, Science and Technology of Japan. *Data deposition:* The atomic coordinates of the *Pyrococcus horikoshii* (*Pho*) CutA in 3 M GdnHCl were deposited in the Protein Data Bank (ID codes 1UMJ).

* Corresponding authors. Fax: +81 22 217 7276 (K. Tsumoto).
E-mail addresses: tsumoto@mail.tains.tohoku.ac.jp (K. Tsumoto), tarakawa2@aol.com (T. Arakawa).

0006-291X/$ - see front matter © 2004 Elsevier Inc. All rights reserved.
doi:10.1016/j.bbrc.2004.08.081

proteins [1,2]. The molecular basis for denaturation by these reagents has been generally attributed to direct ligand binding [3–8] or the effects of the denaturants on the structure and dynamics of solvent water molecules [3,9–13]. Unfolding of proteins by denaturant is driven by the increased surface area upon unfolding [14,15]. These denaturants can influence not only the protein stability, but also the ensemble of the native structure. In this regard, high resolution structure analysis would be informative, although only a few studies have used X-ray diffraction or NMR to probe the effects of denaturants on protein structure [16–20].

Hyperthermophilic proteins show high tolerance to denaturants due to a drastically slow unfolding rate [21], which makes them suitable for elucidating the effects of denaturants on native proteins under non-denaturing condition. Here we attempted to deduce the structural implications from the crystal structure in the native state and 3 M GdnHCl, i.e., the interaction of the denaturant with the native protein and perturbation of the protein structure by the bound denaturant. We chose a hyperthermophilic protein, *Pho*CutA, as a model protein, since it maintains an apparent native structure in 8 M GdnHCl. CutA is a protein that appears to be related to divalent cation homeostasis and is found universally from bacteria to mammals [22–27]. This study reports the crystal structure of the protein in 3 M GdnHCl, where many proteins undergo a major conformational transition from the native to unfolded state.

Materials and methods

Spectroscopic techniques. Expression and purification of *Pho*CutA was in principle followed by Tanaka et al. [26]. To compare the effects of GdnHCl on thermophilic and non-thermophilic proteins, purified and concentrated *Pho*CutA or *Escherichia coli* CutA were diluted in 50 mM Tris–HCl (pH 8.0) buffer containing various concentrations of GdnHCl (0–8 M). After 1 month, tryptophan fluorescence emission and CD spectra were measured. Tryptophan fluorescence emission spectra were measured in an RF-5300PC spectrofluorophotometer (Shimadzu, Japan; quartz cuvette, 1-cm path length, 295-nm excitation wavelength) and were recorded from 300 to 440 nm at 1-nm sampling intervals. Far-UV CD spectra were measured in an AVIV circular dichroism spectrometer (Proteiron, USA): path length, 1.0 mm; resolution, 0.2 nm; and average time, 4 s. The results are expressed as the mean residue ellipticity (θ).

Crystallization of PhoCutA in 3 M GdnHCl. Purified *Pho*CutA was dialyzed against 6 M GdnHCl, 20 mM Tris–HCl (pH 8.0) for more than a week and then concentrated to 20 mg mL^{-1}. Crystallization of *Pho*CutA was performed by the oil-batch method [28]. Three microliters of concentrated *Pho*CutA in 20 mM Tris–HCl (pH 8.0), 6 M GdnHCl was mixed with an equal volume of 100 mM acetate buffer (pH 4.0), 20% (w/v) polyethylene glycol 4000, and 200 mM ammonium sulfate, on 96-microwell plates, then covered with 10 μL of paraffin oil, so the final mother liquor contained 3 M GdnHCl. Diffraction-quality crystals were obtained 1 day after setup.

Diffraction data collection and processing. Diffraction data to a resolution of 1.6 Å were collected on the beamline BL38B1 of SPring-8 (Harima, Japan) under cryogenic conditions with 0.9 Å radiation. The diffraction data were indexed, integrated, scaled, and merged by using the HKL2000 program package [29]. The crystal of *Pho*CutA in 3 M GdnHCl was found to belong to space group $P3$ with unit cell parameters $a = b = 53.2$ and $c = 59.7$ Å.

Structure solution and refinement. The structure of *Pho*CutA in 3 M GdnHCl was determined at 1.6-Å resolution by the molecular replacement method with the program AMoRe [30], using the structure of Se-Met-substituted *Pho*CutA (PDB code, 1j2v) as a search probe. The complete atomic model with a total of 101 residues including side chains was rebuilt manually with the molecular graphics program O [31].

Positional and individual *B*-factor refinement was carried out with the program CNS [32]. To monitor the refinement, a random 10% subset of all reflections was set aside for calculation of the free *R* factor (R_{free}). Topology and parameter files for the guanidine molecule were obtained from the Heterocompound Information Center of Uppsala (HIC-Up) on the Uppsala website [33]. Because the guanidine molecules were found on the crystallographic 3-fold axis of symmetry, the occupancies of all atoms of the guanidine were set to 0.33. After iterative cycles of refinement and manual model fitting, water molecules were automatically located by peak-searching on the SIGMAA-weighted mF_o–DF_c map [34], and some of the water molecules, which occupied irrelevant positions, were deleted on the basis of the real-

Table 1
Data collection and refinement statistics

Data collection	
Space group	$P3$
Cell dimensions (Å)	$a = b = 53.2$, $c = 59.7$
Beamline	BL38B1
Resolution (Å)[a]	40–1.60 (1.66–1.60)
Wavelength (Å)	0.9000
R_{sym} (%)[a,b]	3.9 (22.1)
Completeness (%)[a]	99.6 (100.0)
Observed reflections	94387
Unique reflections	24828
$I/\sigma(I)$	19.9
Multiplicity[a]	3.9 (3.8)
Refinement and model quality	
Resolution range (Å)	20–1.6
No. of reflections	24850
R-factor[c]	0.214
R_{free} factor[d]	0.253
Total protein atoms	1726
Total ligand atoms	16
Total water atoms	125
Average *B*-factor (Å^2)	21.1
Rms deviation from ideality	
Bond lengths (Å)	0.017
Bond angles (°)	1.703
Improper angles (°)	22.70
Dihedral angles (°)	1.119
Ramachandran plot (%)	
Residues in most favored regions	95.2
Residues in additional allowed regions	4.8
Residues in generously allowed regions	0.0

[a] The values in parentheses refer to data in the highest resolution shell.

[b] $R_{sym} = \sum_h \sum_i |I_{h,i} - \langle I_h \rangle| / \sum_h \sum_i |I_{h,i}|$, where $\langle I_h \rangle$ is the mean intensity of a set of equivalent reflections.

[c] *R*-factor $= \sum |F_{obs} - F_{calc}| / \sum F_{obs}$, where F_{obs} and F_{calc} are observed and calculated structure factor amplitudes.

[d] R_{free}-factor was calculated for *R*-factor, with a random 10% subset from all reflections.

space correlation coefficient and/or the maximum density level, using the procedure in the program CNS [32]. The crystallographic R values (R_{free} values) finally converged to within 21.4% (25.3%). The stereochemical quality of the final refined models was analyzed with the program PROCHECK [35]. Figures are produced with MOLSCRIPT [36]. The parameters regarding the data collection and reduction are shown in Table 1.

Results and discussion

Spectroscopic study

In GdnHCl-free solution, the tryptophan fluorescence spectrum of *Pho*CutA had a peak at 342 nm. No red-shift of tryptophan fluorescence was observed even in 3 or 8 M GdnHCl solutions (Fig. 1), indicating that denaturation, which would cause exposure of buried tryptophans to the aqueous environment and hence result in red-shift in fluorescence emission, did not occur. However, the fluorescence intensity was increased at higher GdnHCl concentrations, suggesting that the fluorescence quenching of some tryptophan residues was relieved by GdnHCl.

The mean residue ellipticity at 222 nm of *Pho*CutA in various GdnHCl concentrations showed no changes in secondary structure even at 8 M GdnHCl (CD data not shown). This preservation of CD intensity indicates that *Pho*CutA has a rather rigid secondary structure. We incubated *Pho*CutA in 8 M GdnHCl for a month and found that the secondary structure was still maintained (CD data not shown).

Crystal structure of PhoCutA in 3 M GdnHCl

To analyze the effects of GdnHCl on the structure of *Pho*CutA, we crystallized *Pho*CutA in a solution containing 3 M GdnHCl. Purified *Pho*CutA was dialyzed against 6 M GdnHCl for a week and then subjected to crystallization trials after concentration to 20 mg mL^{-1}. The oil-batch method [28] was used for crystallization, so the final concentration of GdnHCl was 3 M. The crystal structure of *Pho*CutA in 3 M GdnHCl was determined at 1.6-Å resolution by the molecular replacement method using native *Pho*CutA (PDB code, 1j2v) as a search model.

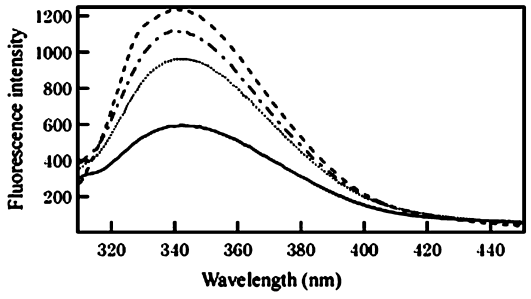

Fig. 1. Tryptophan fluorescence spectra of *Pho*CutA in 0 M (—), 3 M (· · · · · ·), 6 M (–·–), and 8 M (– – –) GdnHCl.

The overall structure of *Pho*CutA in 3 M GdnHCl is identical to the native structure (Fig. 2A). *Pho*CutA has a large number of intramolecular hydrogen bonds in the native state, of which 92.5% and 83.8% of hydrogen bonds with distances $\leqslant$3.0 and $\leqslant$3.3 Å were retained in 3 M GdnHCl. The hydrogen bonds that disappeared from the structure in 3 M GdnHCl were located mainly on the surface (Fig. 2B), suggesting interactions between peptide groups and GdnHCl. However, no electron density of GdnHCl around the peptide groups was observed.

Crystal structure of the native *Pho*CutA shows that the protein has seven ion pairs per monomer (Glu24–Arg68, Glu99–Arg25, Glu63–Lys66, Glu64–Lys101, Glu71–Arg68, Asp60–Arg58, and Asp84–Arg82), whose distances are all $\leqslant$3.0 Å, and which are all located on the protein surface. All these ion pairs were present even in 3 M GdnHCl, in spite of their location at protein surface. The average RMS deviations of residues that participated in ion pairs were 0.27 and 0.71 Å for side chain and Cα atoms, respectively, although those of Glu, Asp, Lys, and Arg, which cannot contribute to ion pairing, were 0.49 and 2.12 Å for side chain and Cα atoms, respectively.

$GdnH^+$ binds to the peptide groups and hence competes with intramolecular hydrogen bonds. Being ionic, $GdnH^+$ weakens ion pairs due to electrostatic stabilization of the charges. The observed marginal effects of GdnHCl on the intramolecular hydrogen bonds and ion pairs in *Pho*CutA indicate that these intramolecular interactions are unusually stable, suggesting that the crystal structure of *Pho*CutA is suitable for discussion about the effects of $GdnH^+$ on the protein surface under non-denaturing condition.

Perturbation of side chains of Trp residues by GdnHCl

Although CD shows no apparent changes, there are local perturbations in the *Pho*CutA structure by 3 M GdnHCl, consistent with the fluorescence data. As described above, some surface hydrogen bonds are lost in 3 M GdnHCl. A local structural difference in the main chain was observed in a loop from Tyr39 to Lys44 in the presence of 3 M GdnHCl (Fig. 3), as demonstrated by perturbation of electron density in the loop region of Tyr39–Lys44. Nevertheless, positions of other residues were quite clear. Relative values of temperature factor (B-factor) were increased around the loop (Fig. 4). These results indicate that the main-chain mobility of this region is higher than the rest of the protein. According to Nozaki and Tanford [37], tryptophan is five times more soluble in 6 M GdnHCl than in GdnHCl-free solution; the greatest difference in solubility among the amino acids they measured. Aromatic amino acids have been

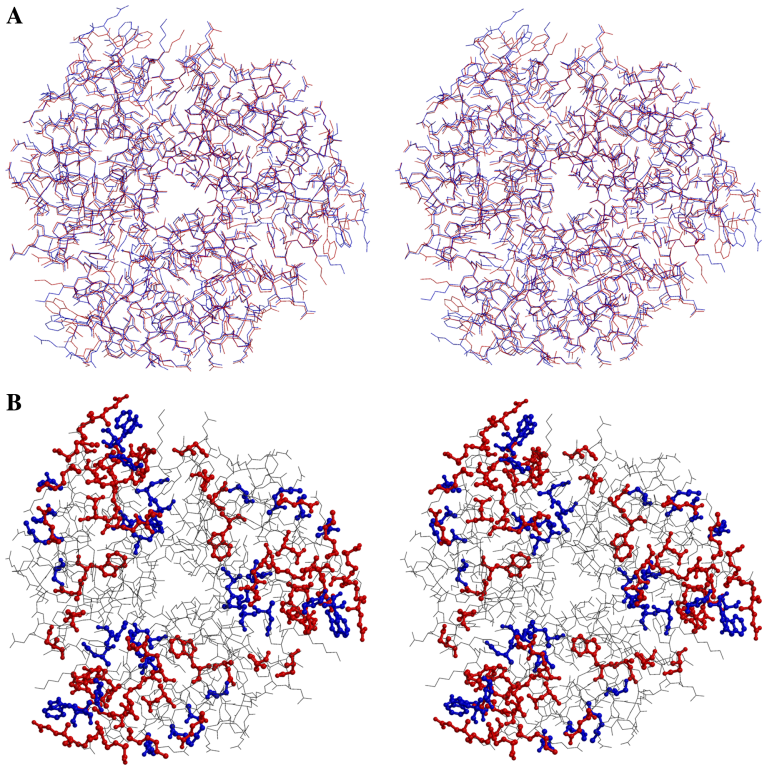

Fig. 2. Crystal structure of *Pho*CutA in 3 M GdnHCl. (A) Superposition of the trimeric structure of *Pho*CutA in 3 M GdnHCl (magenta) and without GdnHCl (blue). (B) Hydrogen bonds disappeared from the *Pho*CutA structure in 3 M GdnHCl. Hydrogen bonds with distances $\leqslant$3.0 Å disappeared in 3 M GdnHCl structure are shown with red ball-and-stick styles, and $\leqslant$3.3 Å are shown with blue.

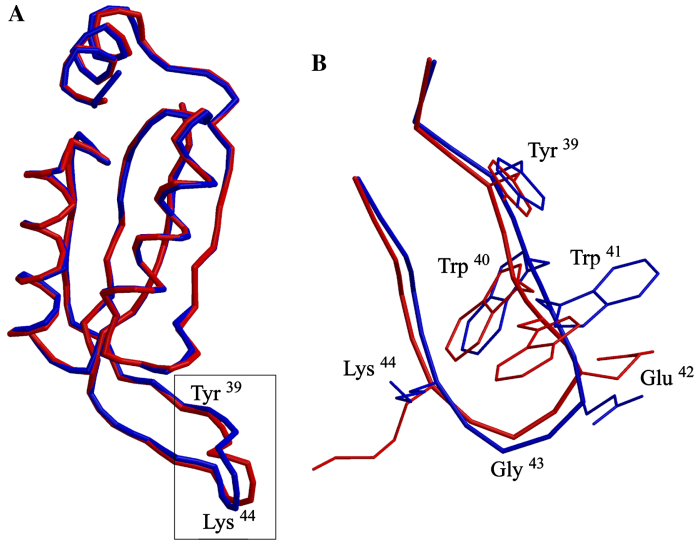

Fig. 3. Superposition of the *Pho*CutA monomer structures in 0 (blue) and 3 M (red) GdnHCl. (A) Cα traces of complete monomer chains. (B) Cα traces and side chains of the loop from Tyr39 to Lys44 (magnified view of the boxed area in A).

implicated as the major binding sites for GdnHCl [37,38]. Our fluorescence and crystal structure results reflect the effects of GdnHCl on surface tryptophans. CH–π interactions [39] can contribute to the interaction of Trp with GdnHCl, although little electron density due to 3 M GdnHCl was observed near the Trp residues. The absence of electron density suggests that binding of GdnHCl to the loop, possibly Trp residues, is neither stoichiometric nor specific, yet is sufficient to cause structural perturbation of the loop. Specific binding of GdnHCl with a Trp residue via hydrogen bond formation has been observed in the crystal structure of hen

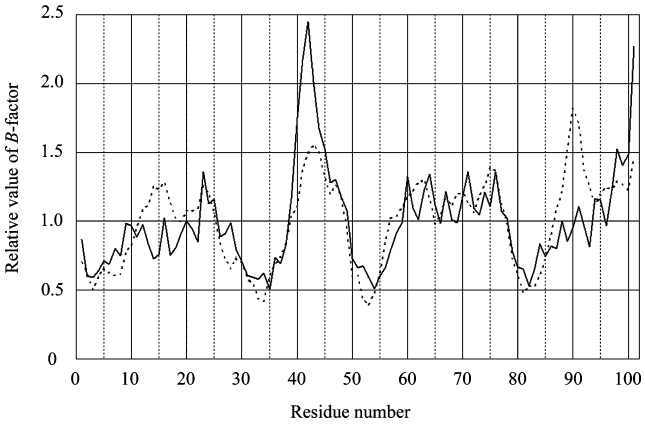

Fig. 4. Superimposed plots of the main-chain *B*-factors for the *Pho* CutA structures in 3 M GdnHCl (solid line) and without GdnHCl (dotted line). The plotted values are relative to the average of all values.

lysozyme with 1.2 M GdnHCl [17]; however, to the best of our knowledge, this is the first report of structural perturbation via effects of GdnHCl on the surface Trp residues.

Specific binding of $GdnH^+$ to Asp residues and main chain

In the refined structure, two $GdnH^+$ ions were located in the center hole of the trimer, precisely on the crystallographic 3-fold axis (Fig. 5A). The SIGMAA-weighted mF_o–DF_c electron density map around the $GdnH^+$ molecule was illustrated in Fig. 5B. The specific binding site of $GdnH^+$ ions is present in one folded protein and is not introduced by crystal packing. The nitrogen atoms of the two $GdnH^+$ ions interact with a total of nine oxygen atoms: Oδ1 and Oδ2 in Asp86 and O in Asp84 in each of the three monomers (Fig. 5). The distances between a nitrogen and Oδ1 and Oδ2 in Asp86 and O in Asp84 are 2.85, 3.04, and 3.10 Å, respectively. In the absence of GdnHCl, these oxygen atoms are hydrogen bonded with water molecules. There is considerable precedent for this coordination, since in the structures of protein complexes with GdnHCl reported so far, some of the nitrogen atoms of GdnHCl interact with oxygen atoms [16–20]. The atomic *B*-factor values of $GdnH^+$ and its interacted atoms of protein molecules are summarized in Table 2.

The overall *B*-factors of ribonuclease A and hen lysozyme have been reduced in denaturants [16,17,19]. On the contrary, those of *Pho*CutA in 3 M GdnHCl were almost the same as in the native structure. The atomic *B*-factors in the vicinity of the $GdnH^+$ binding site are relatively low (Fig. 4), as is the case for hen lysozyme crystallized in 1.2 M GdnHCl [17] and for ribonuclease A crystallized in 0.7 M GdnHCl [16]. The relatively low *B*-factors in the region around Asp86 suggest that binding of GdnHCl to this site is rather specific. The *B*-factor values for Asp86–Trp95 which locate in β strand 5 and the N terminus of helix 3 were markedly reduced by GdnHCl (Fig. 4). The observed low *B*-factor around Asp86 in 3 M GdnHCl suggests the stabilization of this region by the bound $GdnH^+$ ions.

Although the gross structure is unaltered by 3 M GdnHCl, local structures are altered as described above, most likely reflecting an alteration of the conformational ensemble toward more disordered local structures. The present results indicate a possibility that optimized charge–charge interactions provide structural determinants for enhanced stability of proteins from thermophilic organisms [40,41].

GdnHCl binding

As described above, there are two modes of $GdnH^+$ bindings: the specific bindings of $GdnH^+$ with some acidic residues and non-specific bindings around Trp residues and peptide groups on the protein surface. It

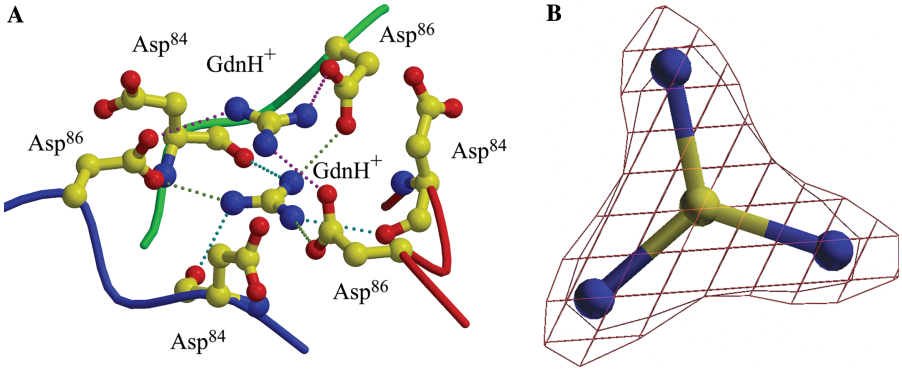

Fig. 5. The bound $GdnH^+$ molecules. (A) Direct $GdnH^+$ binding site in the structure in 3 M GdnHCl. The two molecules of $GdnH^+$ and the nearby residues are shown in ball-and-stick style. (B) The early SIGMAA-weighted mF_o–DF_c electron density map around the $GdnH^+$ molecule contoured at 3.2σ. Because the $GdnH^+$ model is not included in the model refinement, the map is less biased by the $GdnH^+$ model. The final refined model is also displayed.

Table 2
B-factor values of $GdnH^+$ and its interacted atoms of protein molecules

Molecule name (molecular number)[a]	Atom	*B*-factor (Å^2)
$GdnH^+$ molecules		
$GdnH^+$(1001)[a]		
	C	31.66
	N1	30.94
	N2	30.71
	N3	30.08
$GdnH^+$(1002)[a]		
	C	29.01
	N1	32.52
	N2	32.87
	N3	33.27
$GdnH^+$(1003)[a]		
	C	28.80
	N1	29.82
	N2	30.21
	N3	29.53
$GdnH^+$(1004)[a]		
	C	32.35
	N1	35.89
	N2	36.16
	N3	36.25
Counterpart atoms		
Asp86 (chainA)[a]	Oδ2	20.52
Asp86 (chainA)[a]	Oδ1	21.20
Asp84 (chainA)[a]	O	15.58
Asp86 (chainB)[a]	Oδ2	21.33
Asp86 (chainB)[a]	Oδ1	22.65
Asp84 (chainB)[a]	O	14.79

[a] The number of $GDNH^+$ in parantheses (1001–1004) and the chain name (A and B) correspond to those given in deposited PDB file (IUMJ).

is evident that binding of GdnHCl to the native protein is limited, resulting in local structural perturbation. Binding of denaturant molecules is structure- and concentration-dependent ([15,42], Arakawa and Timasheff, unpublished results) with a greater binding at higher denaturant concentrations and for the unfolded state. Since the *Pho*CutA seems to maintain the native structure up to 8 M GdnHCl, a low number of $GdnH^+$ binding is expected. The electron density of GdnHCl was observed only in the center hole. Binding of GdnHCl around Trp residues and peptide groups was inferred from the perturbation of electron density of the Trp residues and from the loss of surface intramolecular hydrogen bonds. In relation to the denaturing action, binding of $GdnH^+$ can be defined as preferential interactions. Preferential interactions are a measure of both solute binding, ranging from stoichiometric and tight bindings to transient retardations of solute diffusion by the protein surface, and water binding. A rather large binding of $GdnH^+$ to the native protein has been observed by equilibrium dialysis or isopiestic equilibrium measurements [15,42–44]. The absence of extensive site binding of $GdnH^+$ ions observed here suggests that most of the bindings observed by preferential interaction measurements reflect those of transient ones. Therefore, the perturbation of electron density of Trp residues and the loss of surface hydrogen bonds are most likely due to the transient bindings of GdnHCl.

Conclusion

The following structural features were observed by comparing the crystal structures of the protein in 0 and 3 M GdnHCl: relatively small number of structurally perturbed residues, breakage of only about 10% of the large number of short intramolecular hydrogen bonds (distance shorter than 3.0 Å), complete conservation of salt bridges on the protein surface, and binding of two $GdnH^+$ ions in the cavity of the protein trimer. The effects of the denaturant on the structure of *Pho*CutA and binding of $GdnH^+$ were rather limited; specific binding around an acidic residue and non-specific binding around tryptophan residues and surface peptide bonds involved in hydrogen bonding.

Acknowledgments

We thank K. Miura of the Japan Synchrotron Radiation Research Institute (JASRI) for her help in X-ray diffraction experiments at SPring-8. We also thank Drs. K. Yutani and K. Ogasahara of Osaka University in Japan for their helpful suggestions.

References

[1] C.N. Pace, Determination and analysis of urea and guanidine hydrochloride denaturation curves, Methods Enzymol. 131 (1986) 266–280.
[2] C.L. Tsou, Inactivation precedes overall molecular conformation changes during enzyme denaturation, Biochim. Biophys. Acta 1253 (1995) 151–162.
[3] B.J. Bennion, V. Daggett, The molecular basis for the chemical denaturation of proteins by urea, Proc. Natl. Acad. Sci. USA 100 (2003) 5142–5147.
[4] J.A. Schellman, Solvent denaturation, Biopolymers 17 (1978) 1305–1322.
[5] J.A. Schellman, Selective binding and solvent denaturation, Biopolymers 26 (1987) 549–559.
[6] T. Arakawa, S.N. Timasheff, Protein stabilization and destabilization by guanidinium salts, Biochemistry 23 (1984) 5924–5929.
[7] G.I. Makhatadze, P.L. Privalov, Protein interactions with urea and guanidinium chloride—A calorimetric study, J. Mol. Biol. 226 (1992) 491–505.
[8] J.W. Wu, Z.X. Wang, New evidence for the denaturant binding model, Protein Sci. 8 (1999) 2090–2097.
[9] D.B. Wetlaufer, S.K. Malik, L. Stoller, R.L. Coffin, Nonpolar group participation in denaturation of proteins by urea + guanidinium salts. Model compound studies, J. Am. Chem. Soc. 86 (1964) 508–514.

[10] Q. Zou, S.M. Habermann-Rottinghaus, K.P. Murphy, Urea effects on protein stability: hydrogen bonding and the hydrophobic effect, Proteins: Struct. Funct. Genet. 31 (1998) 107–115.
[11] Q. Zou, B.J. Bennion, V. Daggett, K.P. Murphy, The molecular mechanism of stabilization of proteins by TMAO and its ability to counteract the effects of urea, J. Am. Chem. Soc. 124 (2002) 1192–1202.
[12] R. Breslow, T. Guo, Surface-tension measurements show that chaotropic salting-in denaturants are not just water-structure breakers, Proc. Natl. Acad. Sci. USA 87 (1990) 167–169.
[13] G.R. Hedwig, T.H. Lilly, H. Linsdell, Calorimetric and volumetric studies of the interactions of some amides in water and in 6 mol dm^{-3} aqueous guanidinium, J. Chem. Soc. Faraday Trans. 87 (1991) 2975–2982.
[14] E.S. Courtenay, M.W. Capp, R.M. Saecker, M.T. Record Jr., Thermodynamic analysis of interactions between denaturants and protein surface exposed on unfolding: interpretation of urea and guanidinium chloride *m*-values and their correlation with changes in accessible surface area (ASA) using preferential interaction coefficients and the local-bulk domain model, Proteins. Struct. Funct. Genet. Suppl. 4 (2000) 72–85.
[15] S.N. Timasheff, G. Xie, Preferential interactions of urea with lysozyme and their linkage to protein denaturation, Biophys. Chem. 105 (2003) 421–448.
[16] J. Dunbar, H.P. Yennawar, S. Banerjee, J. Luo, G.K. Farber, The effect of denaturants on protein structure, Protein Sci. 6 (1997) 1727–1733.
[17] S.C. Mande, M.E. Sobhia, Structural characterization of protein-denaturant interactions: crystal structures of hen egg-white lysozyme in complex with DMSO and guanidinium chloride, Protein Eng. 13 (2000) 133–141.
[18] F. Arnesano, L. Banci, I. Bertini, D. Koulougliotis, Solution structure of oxidized rat microsomal cytochrome *b*5 in the presence of 2 M guanidinium chloride: monitoring the early steps in protein unfolding, Biochemistry 37 (1998) 17082–17092.
[19] A.C.W. Pike, K.R.A. Acharya, structural basis for the interaction of urea with lysozyme, Protein Sci. 3 (1994) 706–710.
[20] D. Shortle, M.S. Ackerman, Persistence of native-like topology in a denatured protein in 8 M urea, Science 293 (2001) 487–489.
[21] K. Ogasahara, M. Nakamura, S. Nakura, S. Tsunasawa, I. Kato, T. Yoshimoto, K. Yutani, The unusually slow unfolding rate causes the high stability of pyrrolidone carboxyl peptidase from a hyperthermophile, *Pyrococcus furiosus*: equilibrium and kinetic studies of guanidine hydrochloride-induced unfolding and refolding, Biochemistry 37 (1998) 17537–17544.
[22] S.T. Fong, J. Camakaris, B.T.O. Lee, Molecular genetics of a chromosomal locus involved in copper tolerance in *Escherichia coli* K-12, Mol. Microbiol. 15 (1995) 1127–1137.
[23] A.L. Perrier, X. Cousin, N. Boschetti, R. Haas, J.M. Chatel, S. Bon, W.L. Roverts, S.R. Pickett, J. Massoulie, T.L. Rosenberry, E. Krejci, Two distinct proteins are associated with tetrameric acetylcholinesterase on the cell surface, J. Biol. Chem. 275 (2000) 34260–34265.
[24] J.L. Burkhead, S.E. Abdel-Ghany, J.M. Morrill, E.A.H. Pilon-Smits, M. Pilon, The *Arabidopsis thaliana* CUTA gene encodes an evolutionarily conserved copper binding chloroplast protein, Plant J. 34 (2003) 856–867.
[25] F. Arnesano, L. Banci, M. Benvenuti, I. Bertini, V. Calderone, S. Mangani, M.S. Viezzoli, The evolutionarily conserved trimeric structure of CutA1 proteins suggests a role in signal transduction, J. Biol. Chem. 278 (2003) 45999–46006.
[26] Y. Tanaka, K. Tsumoto, T. Nakanishi, Y. Yasutake, N. Sakai, M. Yao, I. Tanaka, I. Kumagai, Structural implications for heavy metal-induced reversible assembly and aggregation of a protein: the case of *Pyrococcus horikoshii* CutA, FEBS Lett. 556 (2004) 167–174.
[27] A. Savchenko, T. Skarina, E. Evdokimova, J.D. Watson, R. Laskowski, C.H. Arrowsmith, A.M. Edwards, A. Joachimiak, R.G. Zhang, X-ray crystal structure of CutA from *Thermotoga maritima* at 1.4 Å resolution, Proteins 54 (2004) 162–165.
[28] I. Rayment, Small-scale batch crystallization of proteins revisited: an underutilized way to grow large protein crystals, Structure 10 (2002) 147–151.
[29] Z. Otwinowski, W. Minor, Processing of X-ray diffraction data collected in oscillation mode, Methods Enzymol. 276 (1997) 307–326.
[30] J. Navaza, AMoRe—An automated package for molecular replacement, Acta Crystallogr. A 50 (1994) 157–163.
[31] T.A. Jones, J.Y. Zou, S.W. Cowan, M. Kjeldgaard, Improved methods for building protein models in electron-density maps and the location of errors in these models, Acta Crystallogr. A 47 (1991) 110–119.
[32] A.T. Brunger, P.D. Adams, G.M. Clore, W.L. DeLano, P. Gros, R.W. Grosse-Kunstleve, J.-S. Jiang, J. Kuszewski, M. Nilges, N.S. Pannu, R.J. Read, L.M. Rice, T. Simonson, G.L. Warren, Crystallography & NMR system: a new software suite for macromolecular structure determination, Acta Crystallogr. D 54 (1998) 905–921.
[33] G.J. Kleywegt, T.A. Jones, Databases in protein Crystallography, Acta Crystallogr. D 54 (1998) 1119–1131.
[34] R.J. Read, Improved Fourier coefficients for maps using phases from partial structures with errors, Acta Crystallogr. A 42 (1986) 140–149.
[35] R.A. Laskowski, M.W. MacArthur, D.S. Moss, J.M. Thornton, PROCHECK—A program to check the stereochemical quality of protein structures, J. Appl. Crystallogr. 26 (1993) 283–291.
[36] P.J. Kraulis, MOLSCRIPT—A Program to produce both detailed and schematic plots of protein structures, J. Appl. Crystallogr. 24 (1991) 946–950.
[37] Y. Nozaki, C. Tanford, The solubility of amino acids, diglycine, and triglycine in aqueous guanidine hydrochloride solutions, J. Biol. Chem. 245 (1970) 1648–1652.
[38] C. Tanford, Protein denaturation. C. Theoretical models for the mechanism of denaturation, Adv. Protein Chem. 24 (1970) 1–95.
[39] D.A. Dougherty, Cation–pi interactions in chemistry and biology: a new view of benzene, Phe, Tyr, and Trp, Science 271 (1996) 163–168.
[40] J.M. Sanchez-Ruiz, G.I. Makhatadze, To charge or not to charge?, Trends Biotechnol. 19 (2001) 132–135.
[41] V.V. Loladze, B. Ibarra-Molero, J.M. Sanchez-Ruiz, G.I. Makhatadze, Engineering a thermostable protein via optimization of charge–charge interactions on the protein surface, Biochemistry 38 (1999) 16419–16423.
[42] A.N. Rajeshwara, K.N. Gopalakrishna, V. Prakash, Preferential interaction of denaturants with rice bran lipase, Int. J. Biol. Macromol. 19 (1996) 1–7.
[43] Y. Liu, D.W. Bolen, The peptide backbone plays a dominant role in protein stabilization by naturally occurring osmolytes, Biochemistry 34 (1995) 12884–12891.
[44] J.C. Lee, S.N. Timasheff, Partial specific volumes and interactions with solvent components of proteins in guanidine hydrochloride, Biochemistry 13 (1974) 257–265.